CHAPTER IV
ELECTRICAL PROPERTIES OF A NOVEL LEAD ALKOXIDE PRECURSOR: LEAD GLYCOLATE

4.1 Abstract

The reaction of lead acetate trihydrate $Pb(CH_3COO)_2.3H_2O$ and ethylene glycol, using triethylenetetramine (TETA) as a catalyst, provides in one step an access to a polymer-like precursor of lead glycolate [-$PbOCH_2CH_2O$-]. On the basis of high-resolution mass spectroscopy, chemical analysis composition, FTIR, ^{13}C-solid state NMR and TGA, the lead glycolate precursor can be identified as a trimer structure. The FTIR spectrum demonstrates the characteristics of lead glycolate; the peaks at 1086 and 1042 cm^{-1} can be assigned to the C-O-Pb stretching. The ^{13}C-solid state NMR spectrum gives notably only one peak at 68.639 ppm belonging to the ethylene glycol ligand. The phase transformations of lead glycolate and lead acetate trihydrate to lead oxide, their microstructures and electrical properties were found to vary with increasing temperature. The lead glycolate precursor has superior electrical properties than those of lead acetate trihydrate, suggesting that the lead glycolate precursor can possibly be used as a starting material for producing electrical and semiconducting ceramics, viz. ferroelectric, anti-ferroelectric, and piezoelectric materials.

Keywords: Lead Glycolate, Oxide One Pot Synthesis Process, Electrical Properties, Electrical and Semiconducting Ceramics

4.2 Introduction

Electrical and semiconducting ceramics, such as ferroelectric, antiferro electric, and piezoelectric products, possess a great potential for applications as sensors, actuators, transducers, electro-optic devices, thermistors, resistors and capacitors according to their respective dielectric, pyroelectric and piezoelectric properties [1-4]. The most common and well-known electrical and semiconducting ceramics are lead titanate ($PbTiO_3$), lead zirconate ($PbZrO_3$), lead zirconate titanate (PZT or $Pb(Zr,Ti)O_3$), and lead/lanthanum zirconate titanate (PLZT or $(Pb,La)(Zr,Ti)O_3$) [8]. There are many existing processes used to produce electrical and semiconducting ceramics: the sol-gel method, the chemical co-precipitation, the hydrothermal synthesis, the traditional solid state reaction of mixed oxides, the molten salt preparation, the solvothermal synthesis, the emulsion technique, and the complex polymerization [4-8]. The sol-gel process has advantages over others: a) variety in shapes during the gel-state and low processing temperature, e.g. monoliths, films, fibers, and monosized powders; and b) compositional and microstructural control. In comparison with conventional ceramic raw materials, the starting raw materials of metal alkoxide precursors provide homogeneity and very high purity of metal oxides, even though they are expensive and extremely moisture sensitive.

The methods required for the synthesis of alkoxy derivatives generally depend on their electronegativity and electron configuration. The chelating nature of the glycol and the coordinative saturation achieved by the central atoms in the final products appear to be the main factor for their hydrolytic stability against the hydrolysis and the condensation reaction, and resulting in homogeneous gels rather than precipitates [9]. Other works on metalloglycolates formed from alkaline glycol have also been reported using aluminium, silicon, titanium, and magnesium-aluminium [10-11]. Archer *et al.* [12] studied the role of precursor segregation in the formation of perovskite phase $PbTiO_3$, using lead oxyglycolate $Pb(O_2CCH_2OH)_2$ compound synthesized from refluxing lead carbonate with an appropriate carboxylic acid in water. They suggested that the key to the reaction of $PbTiO_3$ formation was the stoichiometrically controlled "single source" intermediate, $Pb(O_2CCH_2O)_2$ $Ti(OH)_2$, by the elimination of alcohol from hydroxyl protons of the hydroxyl carboxylic ligands and the alkoxide ligands on titanium. The glycolate ligands were

chelated to the lead (II) centre through the carboxylate oxygen and the hydroxyl oxygen atoms. The chelating nature of the under- derivatized glycolate ligand was believed to be an important factor in lowering the pK_a of the hydroxyl proton which promotes reactions with the metal alkoxide compounds.

The oxide one-pot synthesis (OOPS) process is an economic, simple and straightforward process for synthesizing highly moisture stable and pure metal alkoxide precursors using inexpensive and available starting materials, as reported by Wongkasemjit and co-workers [13-15]. In a continuation of the work by Archer *et al.* [12] and Wongkasemjit and co-workers [13-15], the objective of our present work is to synthesize a novel lead glycolate precursor, via the oxide one-pot synthesis (OOPS) process, to be used as a precursor for lead titanate, lead zirconate and lead zirconate titanate. Structural and electrical properties of the lead glycolate precursor were investigated and will be reported here.

4.3 Experimental

Materials

UHP grade nitrogen, 99.99% purity, was obtained from Thai Industrial Gases Public Company Limited (TIG). Lead acetate trihydrate $Pb(CH_3COO)_2.3H_2O$ containing 99.5% purity was purchased from Asia Pacific Specialty Chemical Limited (Australia) and used as received. Ethylene glycol (EG) was purchased from Farmitalia Carlo Erba (Barcelona) and Malinckrodt Baker, Inc. (USA), and purified by fractional distillation under nitrogen at atmospheric pressure, and at 200°C before use. Triethylenetetramine (TETA) was purchased from Facai Polytech. Co., Ltd. (Thailand) and distilled under vacuum (0.1 mm/Hg) at 130°C prior to use. Acetonitrile was purchased from Lab-Scan Co., Ltd., and distilled over calcium hydride powder by the standard technique [15-16].

The starting material, lead acetate trihydrate, was moisture sensitive. Therefore, all glassware used in this experiment was dried in an oven at 110°C overnight prior to use. All syntheses were carried out with a careful exclusion of extraneous moisture by purging with nitrogen.

Instrumental

Fourier transform infrared spectra (FTIR spectrometer) were recorded using (BRUKER,VECTOR 3.0) with a spectral resolution of 4 cm^{-1} using transparent KBr pellets obtained by mixing 0.001 g of a sample with 0.06 g of KBr and hydraulically pressed. ^{13}C-Solid state nuclear magnetic resonance spectrum (^{13}C-NMR) was obtained using a nuclear magnetic resonance analyzer (BRUKER-ADVANCE, DPX-300 MAS-NMR). The positive fast atom bombardment mass spectra (FAB^{+}-MS) were recorded using a proposed structure (Fison Instrument,VG Autospec-ultima 707E) and glycerol as a matrix, a cesium gun as an initiator and cesium iodide (CsI) as a standard for peak calibration. Elemental analysis (EA) was carried out on a C/H/O analyzer (Perkin Elmer, PE 2400 series II). Thermal gravimetric analysis (TGA) was carried out using a Perkin Elmer thermal analysis system with a heating rate of 10°C/min over a 25°-800°C temperature range. Scanning electron micrographs (SEM) were obtained using a SEM micrographer (JEOL, JEOL-5200). X-ray diffraction patterns (XRD) were analyzed using a x-ray diffractometer (Phillip Electronic, N.V. 1999) consisting of CuKα radiation (λ = 0.154nm). Particle size distributions were recorded using a particle sizer (Malvern, Mastersizer X). Electrical properties were obtained using an impedance analyzer (Agilent Technology, 4396B 100 kHz-1.8GHz.).

Lead Glycolate Synthesis

Lead glycolate was synthesized via the OOPS process (eq.1) as follows: a mixture of lead acetate trihydrate ($Pb(CH_3COO)_2.3H_2O$, 0.1 mol, 37.9 g), ethylene glycol (EG, 50 ml.) using triethylenetetramine (TETA, 0.1 mol, 14.6 g) as catalyst was heated at the boiling point of EG under N_2 atmosphere in thermostat oil bath. The excess EG was slowly distilled off to remove water liberated from the reaction. After 1 hr of reaction, the solution color changed from colorless to yellow and golden brown, indicating the completion of the reaction. The reaction mixture was cooled down to obtain a crude precipitate product. The product was purified by washing with acetonitrile. The light silver bronze solid product was obtained, dried in a

vacuum dessicator (0.1 mm Hg) at room temperature, and characterized using FTIR, ^{13}C-NMR, FAB^{+}-MS, TGA and pycnometer.

$$Pb(CH_3COO)_2 .3H_2O + HOCH_2CH_2OH \xrightarrow[200°C]{TETA} -[PbOCH_2CH_2O-]_n- + 3\,H_2O + 2CH_3COOH \quad (eq.1)$$

Electrical Properties

Pellet samples were prepared as a thin disc having a diameter of 12 mm and a thickness of 0.50 mm. We followed the ASTM B263- 94 standard in determining electrical properties: dielectric constant, conductivity, resistivity, loss tangent and dielectric loss. In our experiment, the frequency used was set at 10^6 Hz at room temperature.

4.4 Results and Discussion

The reaction of lead acetate trihydrate and ethylene glycol (EG) using triethylenetetramine as the catalyst can be categorized as a condensation reaction generating water as a by-product [14,15,17]. To force the reaction to go forward, distillation of EG was thus carried out to remove water along with EG from the reaction mixture. The alkoxide precursor was obtained in a silver bronze color [18], and the soft precipitate powder was moisture-stable. To confirm the structure of the product, several common spectroscopic techniques were employed. A FTIR spectrum of lead glycolate along with with a spectrum of lead acetate trihydrate are shown in Fig.4.1. The main characteristic absorbance peaks of the lead glycolate can be seen at 2778-2829, and 1086- 1042 cm^{-1} corresponding to the C-H stretching, and the C-O-Pb stretching of ethylene glycol bidentate ligand, respectively. Our result is consistent with the results obtained by Wang *et al.* and Zeng *et al.* [19-20]. The peak at 573 cm^{-1} clearly shows a typical metal-oxide bond which can be assigned to the O-Pb stretching, consistent with those found by Zerroual and Merkle [21-22] between 200 to 600 cm^{-1} and 400 to 600 cm^{-1}.

Due to the insolubility of the lead glycolate powder in all organic solvents, ^{13}C-NMR solid state mode analysis was carried out and the result is shown in

Fig.4.2. Expectedly, only one single peak at 68.639 ppm, corresponding to ethylene glycol ligand (-PbO$\underline{CH_2CH_2}$O-), is shifted further from the standard peak of ethylene glycol at 63.4 ppm.

Both mass spectroscopy and elemental analyses were also carried out. The results are shown in Tables 4.1 and 4.2, respectively. The proposed fragmentation and structures present in Table1 clearly indicate the trimer of lead glycolate (m/z 801, 55.3%). The C/H percentages from the elemental analysis are 8.864/1.392, very close to 8.990/1.498 calculated theoretically.

Table 4.3 shows the density and average particle size of the lead glycolate precursor; they are 3.02 g/cm^3 and 36.80 microns, respectively. These data can be used in considering a particle packing with other compounds to produce dielectric materials, and in selecting a suitable additive. In term of solubility, the precursor was easily dissolved in acetic acid, sulfuric acid and hydrochloric acid, but mildly in nitric acid.

Thermal behavior was investigated by a TGA measurement. The decomposi tion profile and ceramic yield of the proposed product are shown in Fig. 4.3. The thermal decomposition of the glycol ligand occured in the range of 290°-305°C. The final ceramic yield obtained was 82.50%; this is 1% lower than the theoretical yield value of 83.50% due the evaporation of some lead oxide at around 800°C.

The microstructures of lead acetate trihydrate and lead glycolate, between room temperature and a high temperature using SEM with magnification of 500 at 20 kV, are shown in Fig.4.4. The microstructures of both lead glycolate and lead acetate changed from a plate shape to a spherical shape as temperature was increased.

The phase transformation using the XRD technique can help to explain the phase formation of PbO as a function of temperature (eq.2). We have shown that the oxidation of organic compound occurred at approximately 300°C by the TGA data. However, Ulrich and Wilkinson [23-24] reported that the phase transformation from a red color tetragonal α-PbO into a yellow orthorhombic β-PbO (massicot) occurs at 488°C. In our case, the phase change into α-PbO starts to occur at 400°C for both lead glycolate and lead acetate trihydrate (Figs. 4.5b and 4.5b', respectively), 600°C for mixed phases of α-PbO and β-PbO (Figs.4.5c and 4.5c') and 800°C for β-PbO

(Figs.4.5d and 4.5d'). The XRD patterns obtained at 800°C, indicating β-PbO or the massicotite phase, resemble those recorded at the Joint Committee on Powder Diffraction Standards (JCPDS) number 38-1477 and 05-0570.

$$\text{-[-PbOCH}_2\text{CH}_2\text{O-]-} \longrightarrow \alpha\text{-PbO} \longrightarrow \beta\text{-PbO} \quad \text{(eq.2)}$$

Lead glycolate at room temp., silver bronze color	Red color, tetragonal form at 400°C	Yellow color, massico tite form at 800°C

Electrical property-wise, the Curie temperature is an important factor to determine the switching transition of a structure from a ferroelectric state to a non-ferroelectric state. Dielectric and ferroelectric properties vary significantly above the Curie temperature. At high frequencies, dielectric losses are expected to be low because dipoles do not move at all. Ceramic and polymer materials, normally possessing electrical resistivity values in excess of 10^{11} ohm.m, are used as dielectric materials. Sivan and Ravindran [25] studied dielectric constant and resistivity of PbO and TiO_2 from room temperature to 875 K at 10^5 Hz. They reported that the dielectric constant increased slowly near the Curie temperature, thereafter increased sharply to a maximum value at the Curie temperature, and above this temperature it decreased. This behavior was also found in our case, as can be seen in Fig.4.6 where the dielectric constants increase to maxima at temperature about 600°C and decrease sharply beyond that temperature. Figure 4.7 shows conductivity values of lead glycolate and lead acetate trihydrate. The dielectric constant, resistivity, and conductivity of lead glycolate are 7.42-22.96, 1.3-2.3x10^{11} ohm.m and 4.28-7.99 x 10^{-12} $ohm^{-1}.m^{-1}$, at 10^6 Hz, respectively. The corresponding values of dielectric constant, resistivity, and conductivity for lead acetate trihydrate are 2.5-19.31, na-2.3x10^{11} ohm.m and na-4.40 x 10^{-12} $ohm^{-1}.m^{-1}$, at 10^6 Hz., respectively. Evidently, the electrical properties of lead glycolate are superior than those of lead acetate trihydrate at all temperatures investigated. The decreases in values at 800°C are probably due to the decomposition of lead oxide occurring at high temperature. The data of dielectric constant, conductivity and resistivity of lead glycolate and lead

acetate trihydrate from room temperature to high temperature are summarized in Table 4.4.

From these data, it could be conjectured that the lead glycolate could be used as a better reactant for capacitors or as a ferroelectric material. It is also possible also that the synthesized lead glycolate can be mixed with other oxide compounds to produce superior dielectric constant materials, such as ferroelectric or piezoelectric materials.

4.5 Conclusions

The lead glycolate precursor was successfully synthesized by the "Oxide One Pot Synthesis" process with a very high yield. The product has remarkably high purity as shown by the elemental analysis data, and it is moisture stable as shown by TGA data. The FTIR result shows the Pb-O-C bonds while the NMR data give only one peak of ethylene glycol ligand. FAB^{+}-MS gives the molecular peak of a trimer-[-$PbOCH_2CH_2O$-]$_3$-. Moreover, the percentages of carbon and hydrogen contents in the product are close to the theoretical values. Since the lead glycolate is more stable. It is soluble in most acid solutions, except nitric acid. With its small particle size, lead glycolate is useful for selectively mixing with other precursors such as titanium glycolate and zirconium glycolate to produce lead titanate, lead zirconate and lead titanate zirconate (PZT). From the electrical properties and the microstructures at high temperature, we can summarize the lead glycolate precursor could be used as a possible starting material for ferroelectric, anti-ferroelectric, and piezoelectric materials.

4.6 Acknowledgements

The authors would like to thank Postgraduate Education and Research Program in Petroleum and Petrochemical Technology (ADB) Fund, Ratchadapi sakesompoch Fund, Chulalongkorn University and the Faculty of Engineering, Kasetsart University for the grants provided, and the Department of Materials Engineering, the Chemistry Department and the Physics Department of Kasetsart University, for x-ray microscan, x-ray diffraction, hydraulic pressing and electrical property measurements.

4.7 References

1. J. Fang, J. Wang, J. Mater. Sci. 34 (1999) 1943.
2. P. Lobmann, W. Glaubitt, J. Gross, J. Fricke, J. Non-Cryst. Solids 186(1995) 59.
3. E. C. Paris, E. R. Leite, E. Longo, J. A. Varela, Mater. Lett. 37 (1998) 1.
4. YXL, Sens. and Act. A 35 (1993) 255.
5. J. Fang, J. Wang, L. M. Gan, S.C. Ng, Mater. Lett. 52 (2002) 304.
6. B. A. Hermandez, K. S. Chang, E. R. Fisher, P. K. Dorhout, Chem. Mater. 14(2002) 480.
7. D. Bersani,P.P. Lottici, A. Montenero, S. Pigoni, G. Guappi, J. Non-Cryst. Solids 192-193 (1995) 490.
8. S. R. Gurkovich and J.B. Blum, Am. Ceram. Soc. Bull. 61 (1982) 153.
9. M. Kakihana, T. Okubo, M. Arima, O. Uchiyama, M.Yashima, M. Yoshimura, Chem. Mater. 9/2 (1997) 451.
10. J.Yang, S. Mei, J.M.F. Ferreira, Mater. Sci. Eng. C 15 (2001) 183.
11. V.W. Day, A. Eberspacher, M.H. Frey, W.G. Klemperer, S. Liang, D.A. Payne, Chem. Mater. 8 (1996) 330.
12. L.B. Archer, M.J. Hampden-Smith, E. N. Duesler, Polyhedron 15/5 (1996) 929.
13. K.F. Waldner, R.M. Laine, S. Dhumrongvaraporn (Wongkasemjit), S. Tayaniphan, R. Narayanan, Chem. Mater. 8/12 (1996) 2850.
14. Y. Opornsawad, B. Ksapabutr, S. Wongkasemjit, R. Laine, Eur. Polym. J. 37/9 (2001) 1877.
15. B. Ksapabutr, E.Gulari, S.Wongkasemjit, Mat. Chem. Phys., 83/1(2004), 34.
16. O.Palchik, J. Zhu and A. Gedanken, J.Mater. Chem.,10 (2000) 1251.
17. V.P. Sazonov, et al., J. Phys, Chem. Ref. Data.,31/4 (2002), 989.
18. W. Kwestroo and A. Huizing, J. Inorg. Nucl.Chem., 27(1951), 1951.
19. D. Wang, R. Yu, N. Kumada and N. Kinomura, Chem. Mater., 11/8 (1999), 2008.
20. X. Zeng, Y. Liu, X. Wang Mat. Chem. Phys. 77/1 (2003) 209.
21. L. Zerroual, F. Tedjar, J. Guitton, A. Mousser, J. Pow. Sources 41 (1993) 23
22. R. Merkle, H. Bertagnolli, Polyhedron 18 (1999) 1089.

23. H. Ulrich, P. Berastegui, S. Carlson, J. Haines, J. M. Leger, Angew. Chem. Int. Ed. 40/24 (2001) 4624.

24. T.J. Wilkinson, D.L. Perry, E. Spiller, P. Berdahl, S.E. Derenzo, M.J. Weber, Proceed. Mater. Res. Soc.117 (2002)704.

25. C.G. Sivan Pillai, P.V. Ravindran, Thermochimica 278 (1996) 109.

Captions of Figures and Tables

Figure 4.1 FTIR spectra of the lead acetate trihydrat and lead glycolate precursor.

Figure 4.2 ^{13}C-Solid state NMR spectrum of the synthesized lead glycolate.

Figure 4.3 TGA curve of lead glycolate.

Figure 4.4 The SEM micrographs of lead acetate trihydrate (figures a-d) and lead glycolate (figures a'-d') pyrolyzed at: a) room temperature; b) 400°C; c) 600°C; and d) 800°C.

Figure 4.5 The XRD patterns of lead acetate trihydrate (figures a-d) and lead glycolate (figures a'-d') at: (a) room temp; (b) 400°; (c) 600°; and (d) 800°C.

Figure 4.6 The dielectric constants of lead acetate trihydrate and lead glycolate precursor as unctions of calcined temperature at room temp; 400°; 600°; and 800°C.

Figure 4.7 The conductivity values of lead acetate trihydrate and lead glycolate precursor as functions of calcined temperature at room temp; 400°; 600°; and 800°C.

Table 4.1 The proposed structures and fragments pattern of lead glycolate.

Table 4.2 The percentages of C and H present in the synthesized lead glycolate.

Table 4.3 The physical properties of lead glycolate and lead acetate trihydrate.

Table 4.4 The electrical properties of lead glycolate and lead acetate trihydrate.

Table 4.1 The proposed structures and fragments pattern of lead glycolate.

M/e	% Intensity	Proposed Structures
801	55.3	$-[-PbOCH_2CH_2O-]_3-$
595	25.3	$-OCH_2CH_2OPbOCH_2CH_2OpbOCH_2CH_2O- + H^+$
505	55.7	$-CH_2OPbOCH_2CH_2OPb- + H^+$
45	14.8	$-CH_2CH_2O- + H^+$

Table 4.2 The percentages of C and H present in the synthesized lead glycolate.

(%) Element	Theoretical	Experimental
C	**8.990**	**8.864**
H	**1.498**	**1.392**

Table 4.3 The physical properties of lead glycolate and lead acetate trihydrate.

Powders	Density (g/cm^3)	Average particle size	Solubility
Lead acetate Trihydrate	**2.50**	**100 micron (flake)**	**Methanol, Acetic acid**
Lead glycolate	**3.02**	**36.80 micron**	**Acetic acid, Sulfuric acid, Hydrochloric acid, Nitric acid (slightly)**

Table 4.4 The electrical properties of lead glycolate and lead acetate trihydrate.

Substances	Dielectric constant	Conductivity $(\Omega.m)^{-1}$	Resistivity $\Omega.m$	Loss tangent Tanδ	Dielectric loss
Lead glycolate Room temp.	7.42	4.28×10^{-12}	2.30×10^{11}	0.32	2.40
Lead glycolate 400 °C	16.32	7.28×10^{-12}	1.40×10^{11}	0.20	3.26
Lead glycolate 600 °C	22.96	7.99×10^{-12}	1.30×10^{11}	0.32	7.28
Lead glycolate 800 °C	7.77	2.94×10^{-12}	3.40×10^{11}	0.06	0. 47
Lead acetate trihydrate room temp.	2.50	Na	na	na	na
Lead acetate trihydrate 400 °C	4.99	2.76×10^{-12}	3.60×10^{11}	1.49	7.45
Lead acetate trihydrate 600 °C	19.31	4.40×10^{-12}	2.30×10^{11}	1.11	21.43
Lead acetate trihydrate 800 °C	2.03	1.10×10^{-12}	9.10×10^{11}	0.27	0.54

na means not measurable.

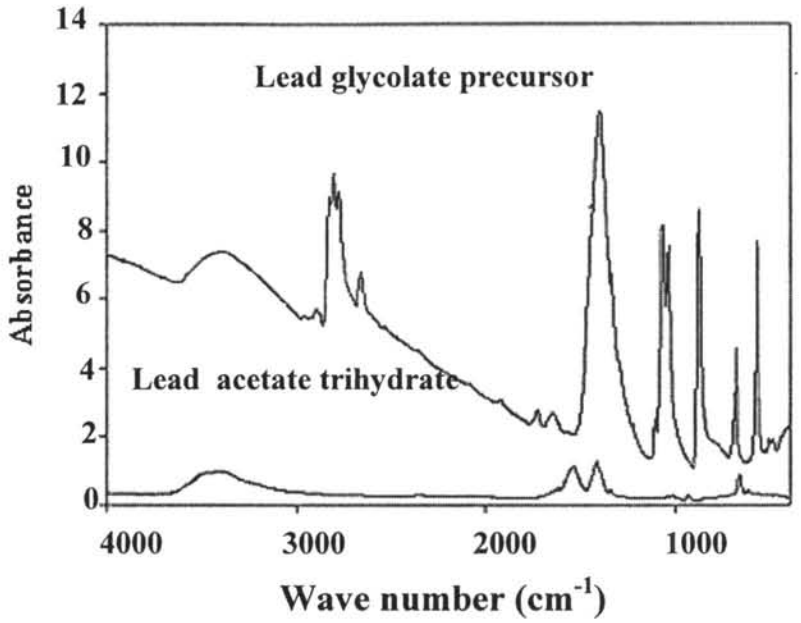

Figure 4.1 FTIR spectra of the lead acetate trihydrat and lead glycolate precursor.

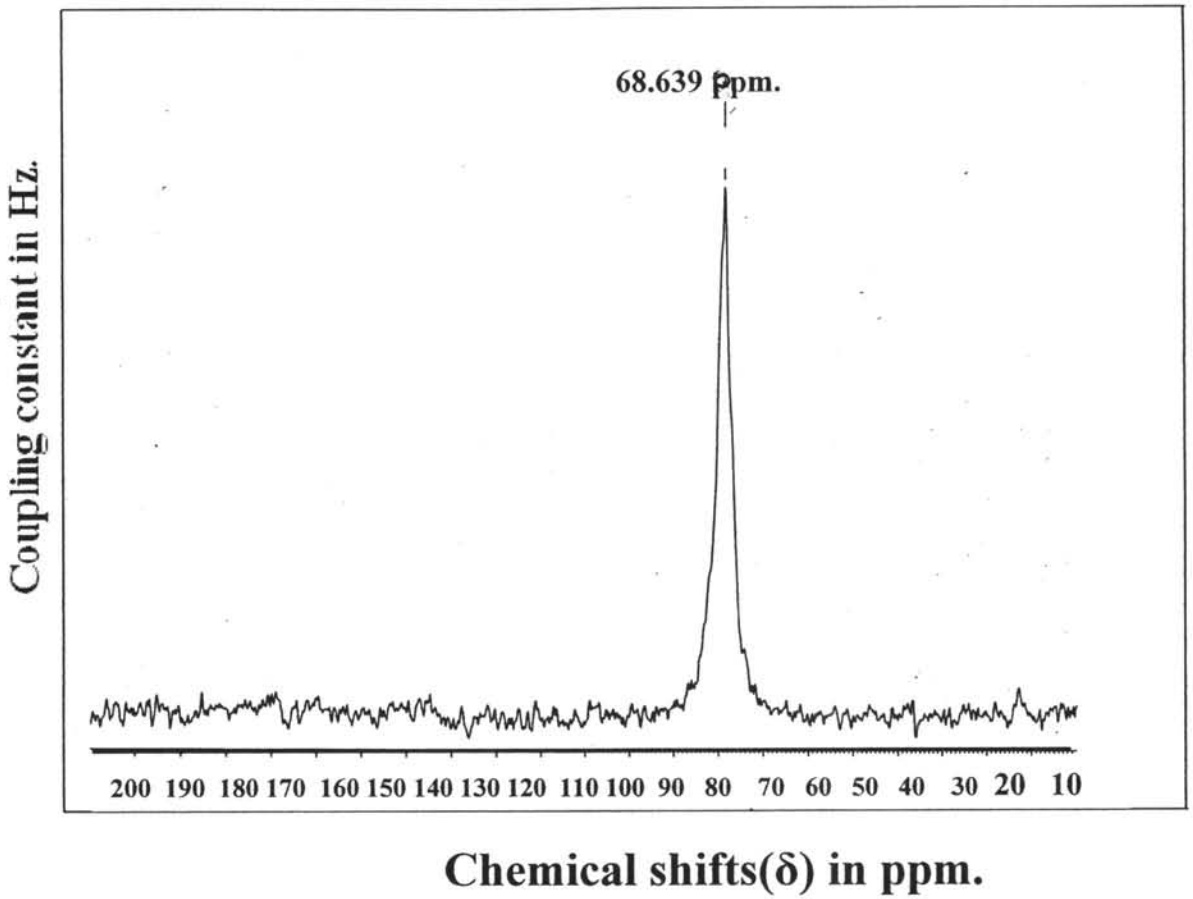

Figure 4.2 ^{13}C-Solid state NMR spectrum of the synthesized lead glycolate.

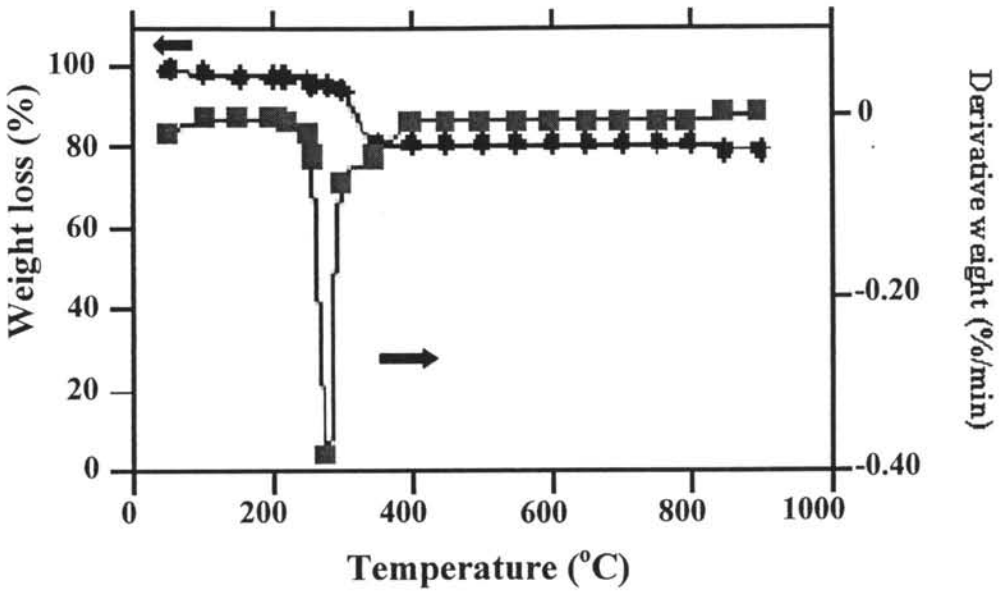

Figure 4.3 TGA curve of lead glycolate.

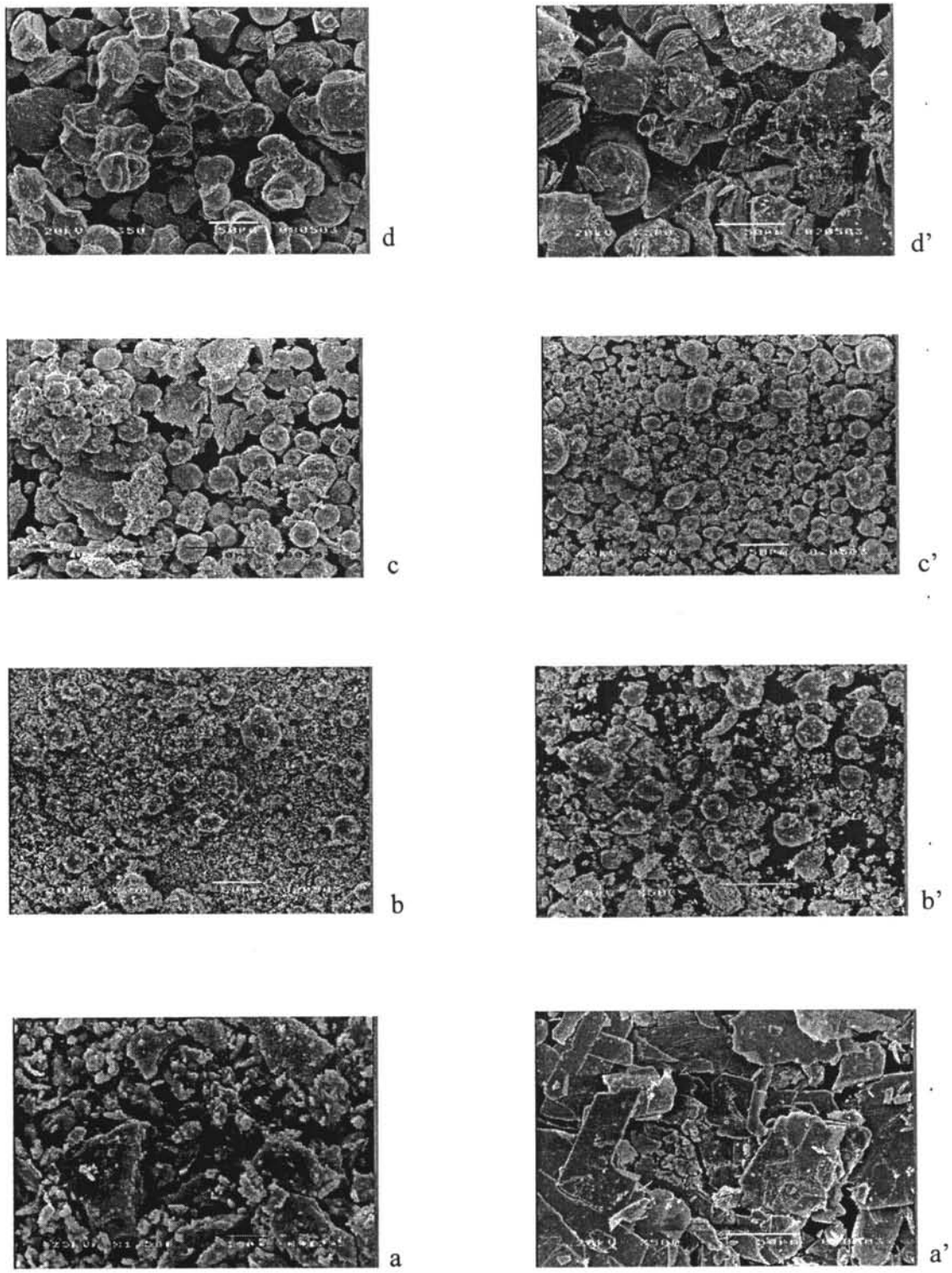

Figure 4.4 The SEM micrographs of lead acetate trihydrate (figures a-d) and lead glycolate (figures a'-d') pyrolyzed at: a) room temperature; b) 400°C; c) 600°C; and d) 800°C.

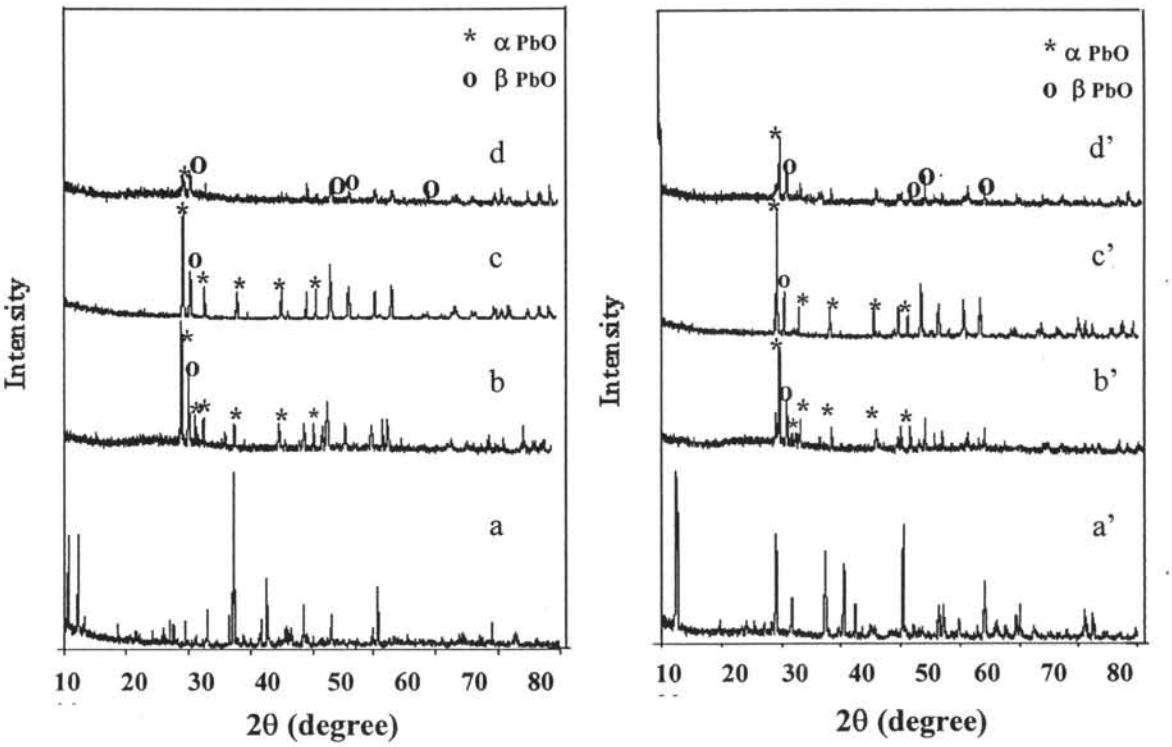

Figure 4.5 The XRD patterns of lead acetate trihydrate (figures a-d) and lead glycolate (figures a'-d') at: (a) room temp; (b) 400°C; (c) 600°C; and (d) 800°C.

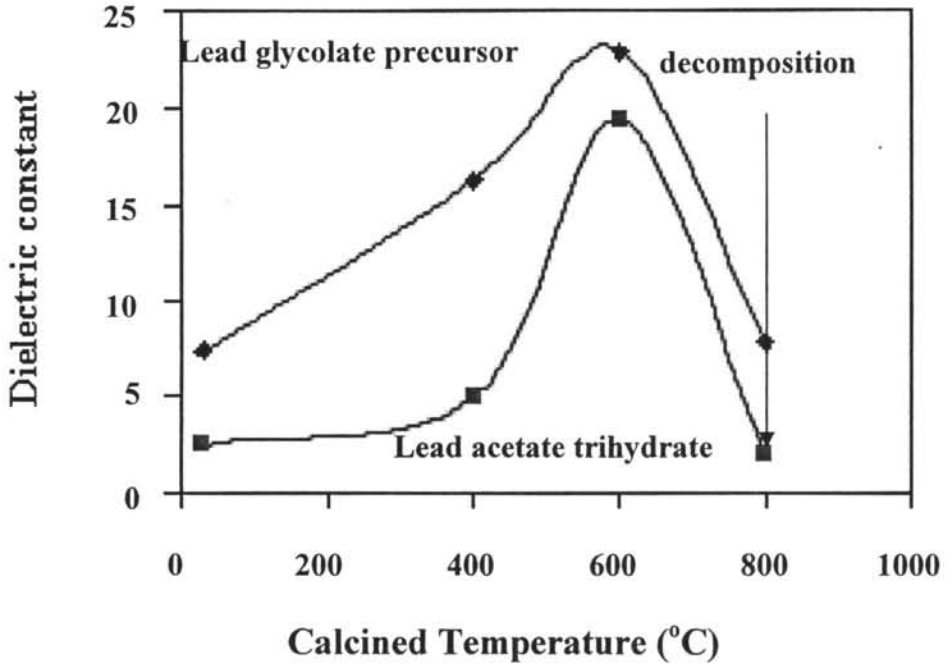

Figure 4.6 The dielectric constants of lead acetate trihydrate and lead glycolate precursor as functions of calcined temperature at room temp; 400°C; 600°C; and 800°C.

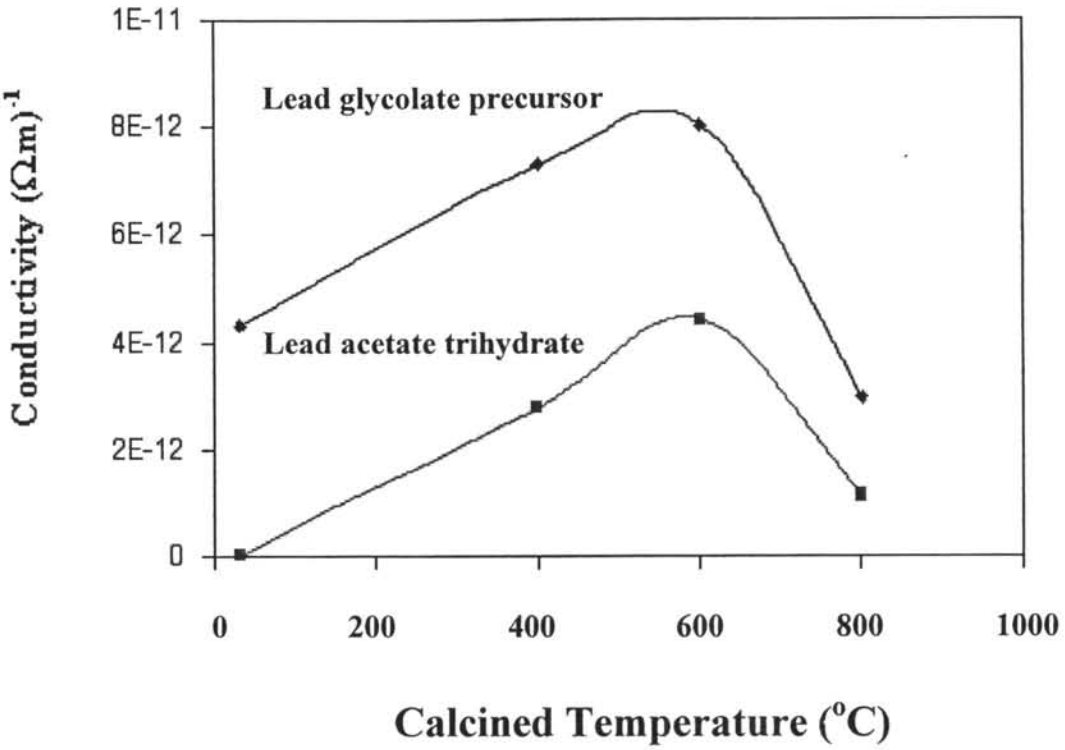

Figure 4.7 The conductivity values of lead acetate trihydrate and lead glycolate precursor as functions of calcined temperature at room temp; 400°C; 600°C; and 800°C.